

White Dwarfs in Open Clusters: Calibrating the Clock

T. von Hippel, D.E. Winget, W.H. Jefferys, and J.G. Scott

*The University of Texas at Austin, 1 University Station C1400, Austin,
TX 78712, USA*

Abstract. We present an update of our on-going effort to improve the precision of white dwarf cosmochronology via careful analyses of white dwarf photometry in open clusters. To improve the precision of white dwarf and main sequence age analysis, we are developing a new interpretative scheme using a Bayesian statistical approach that matches observations to simulated stellar clusters. Here we present our first tests of the Bayesian approach with simulated stellar clusters with ages of 1, 2, and 4 billion years.

1. Introduction

The goal of our open cluster observations and modeling is to improve the precision of white dwarf cosmochronology by comparing white dwarf (WD) cooling ages to main sequence turn-off (MSTO) ages in open clusters spanning a wide range of age and metallicity. Cluster observations to date demonstrate a good overall agreement between WD and MSTO ages for clusters spanning the age range of ~ 160 Myr to ~ 4 Gyr (von Hippel 2005). Our future work will focus on pushing the well observed cluster sample to greater ages, to a wider metallicity range, and to increasing the precision for the cluster WD and MSTO age determinations. Here we focus on our approach to increasing the precision of the age determinations.

2. New Computational Approach

We apply a new modeling plus Bayesian technique to determine precise white dwarf cooling ages and standard stellar evolutionary ages. For the examples here, the ingredients are a Miller & Scalo (1979) Initial Mass Function, Girardi et al. (2000) stellar evolution time scales, the Initial-Final Mass Relation of Weidemann (2000), WD cooling time scales of Wood (1992), and the WD atmosphere colors of Bergeron et al. (1995). Other variants on these modeling ingredients will be incorporated in the future. Our Bayesian approach uses a Markov Chain Monte Carlo scheme to recover the distribution in the parameters of interest, which include masses for every cluster star, as well as the cluster-wide properties of age, distance, metallicity, and reddening.

In Figures 1–3 we present internal validation studies of our technique, in which simulated clusters with different, but known, parameters are presented to the Bayesian code for analysis. In Figure 1 we present a simulated 2 Gyr old star cluster as it might be observed with HST. The location of each star

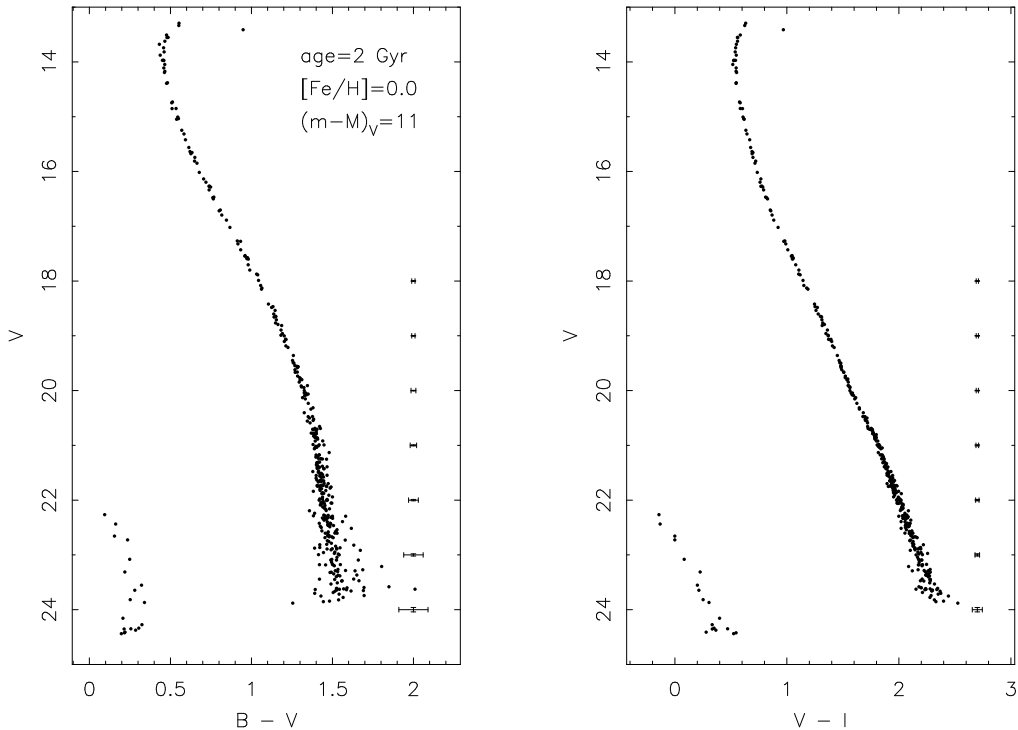


Figure 1. BV and VI color-magnitude diagrams for an example simulated cluster. This cluster is 2 Gyr old, 1.5 kpc distant, has $A_V = 0$, and contains 400 stars, 26 of which are WDs. Photometric errors typical for HST/ACS are included. Average photometric errors as a function of depth are presented in the error bars down the right hand side of each color-magnitude diagram.

in the color-magnitude diagram is determined by randomly drawing it from the IMF, assigning it the properties according to the model ingredients discussed above, then scattering its photometry based on the assumed errors as a function of depth. The number of stars and the errors are set to match those of a good target open cluster in one or two HST/ACS fields. We have not yet incorporated field stars, but this will be done in the future. For some clusters, field stars are not a problem as they can be removed by proper motions and/or radial velocities. For other clusters this will not be possible, and our technique will incorporate the probability of a star being a field star as a function of its location in the color-magnitude diagram.

Our Bayesian approach recovers the probability distributions for the masses of every cluster star. Five representative examples are presented in Figure 2. Note the very high precision (probability distributions with widths of only a few thousandths of a solar mass) in the masses for the main sequence and red giant stars. These are internal measurements of precision, of course, and do not represent the differences between different model isochrones, i.e., these precisions do not represent the external uncertainties in the mass-luminosity relation. The white dwarf masses, particularly as we plot them here, are much less precise,

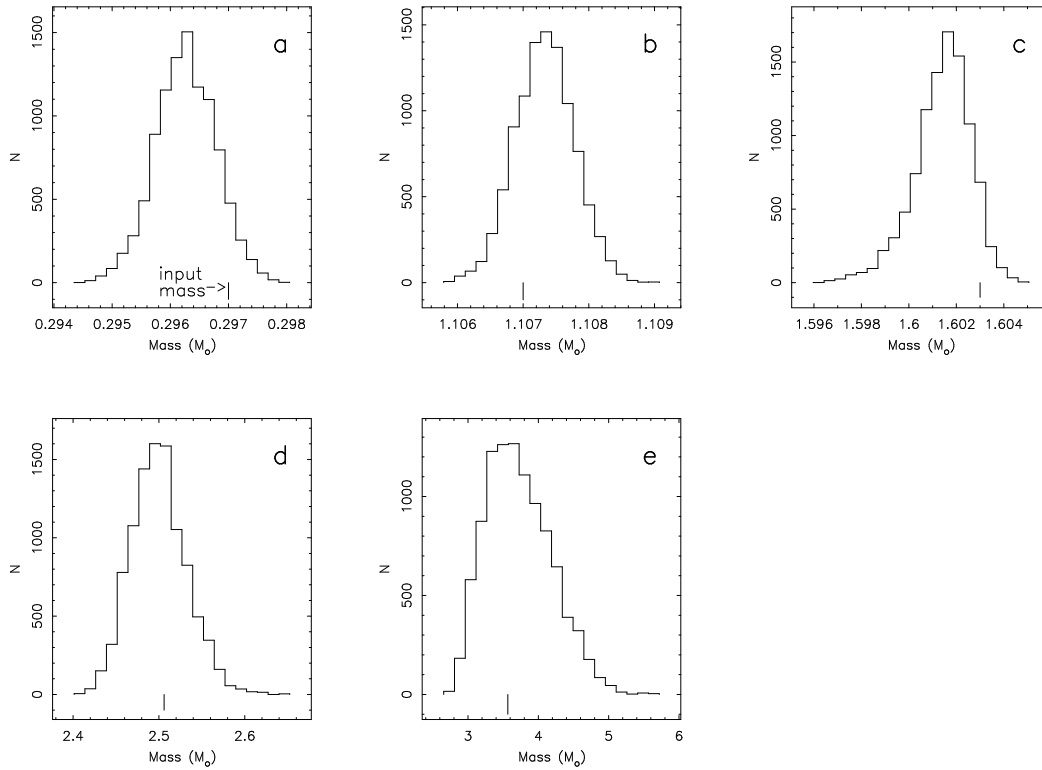


Figure 2. Mass determinations for five example stars from the cluster of Figure 1. Panels *a* and *b* present main sequence stars, panel *c* presents a red giant, and panels *d* and *e* present white dwarfs. The input masses are marked with short vertical lines near the x-axes.

because we plot their zero age main sequence mass and because a wide range in initial masses becomes a narrow range in white dwarf mass.

The goal of our Bayesian analysis is to recover the probability distributions for the cluster ages, and these are presented in Figure 3. For this internal precision study, for the number of cluster stars simulated (400), and for the assumed photometric error bars, the ages are highly precise, with typical age distributions having a width of only 1–5% of the cluster age.

Acknowledgments. We appreciatively acknowledge support for this research from NASA through LTSA grant NAG5-13070.

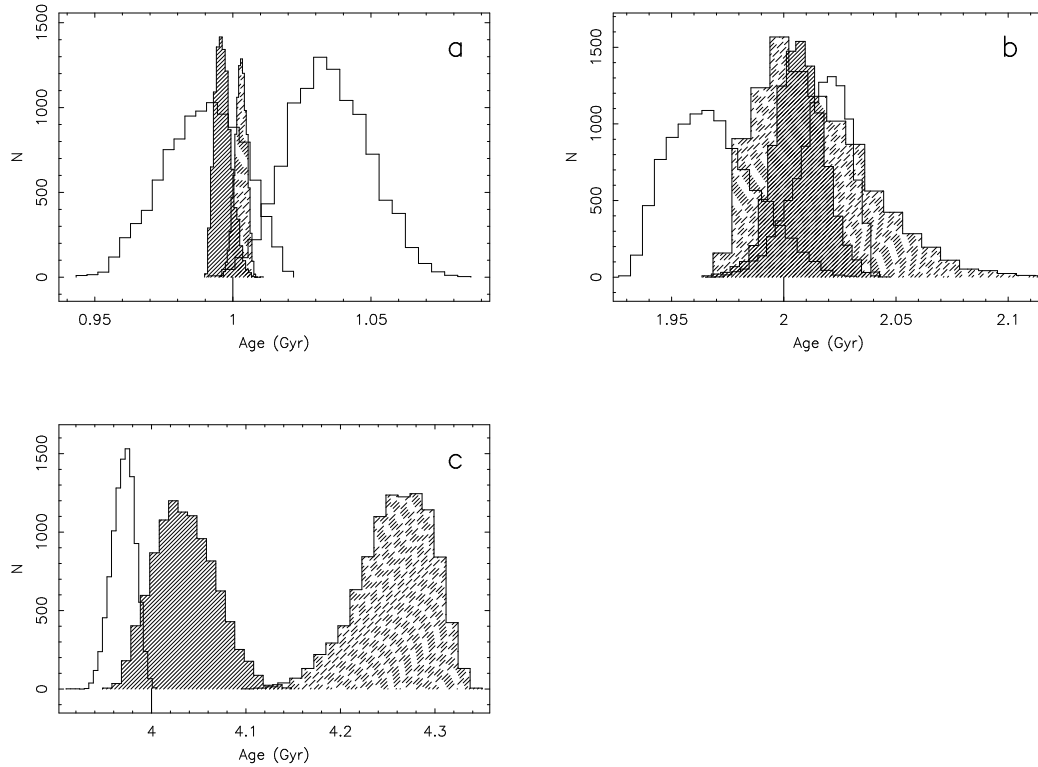


Figure 3. Age determinations for eleven example clusters. There are four simulated clusters at 1 (panel *a*) and 2 Gyr (panel *b*), and three simulated clusters at 4 Gyr (panel *c*). The input ages are marked with short vertical lines near the x-axes. The remainder of the cluster parameters are similar to those for the cluster presented in Figure 1.

References

- Bergeron, P., Wesemael, F., & Beauchamp, A. 1995, *PASP*, 107, 1047
 Girardi, L., Bressan, A., Bertelli, G., & Chiosi, C. 2000, *A&A*, 141, 371
 Miller, G. E., & Scalo, J. M. 1979, *ApJS*, 41, 513
 von Hippel, T. 2005, *ApJ*, submitted
 Weidemann, V. 2000, *A&A*, 363, 647
 Wood, M.A. 1992, *ApJ*, 386, 539